Acta Neuropathol (1993) 86: 215 – 223

Acta Neuropathologica

Regular papers

Posterior cortical atrophy in Alzheimer's disease: analysis of a new case and re-evaluation of a historical report*

P. R. Hof[1,2], N. Archin[1], A. P. Osmand[3], J. H. Dougherty[3], C. Wells[4], C. Bouras[1,5], and J. H. Morrison[1,2]

[1] Fishberg Research Center for Neurobiology, Box 1065, and [2]Department of Geriatrics and Adult Development, Mount Sinai School of Medicine, One Gustave L. Levy Place, New York NY 10029, USA
[3] Division of Neurology, Department of Medicine, University of Tennessee Medical Center, Knoxville, TN 37920, USA
[4] Departments of Psychiatry and Neurology, Vanderbilt University, Nashville, TN 37240, USA
[5] Department of Psychiatry, University of Geneva School of Medicine, IUPG Bel-Air, CH-1225 Chêne-Bourg, Geneva, Switzerland

Received February 10, 1993/Revised, accepted March 25, 1993

Summary. Disturbances of visual function are not uncommon in Alzheimer's disease and several cases with complex impairment of visuospatial abilities have been described. For instance, posterior cortical atrophy has been demonstrated in cases displaying Balint's syndrome as the first symptom of the dementing illness. Such cases showed very high lesion counts in the occipital cortex, as well as in visual association regions in the posterior parietal and posterior cingulate cortex, whereas the prefrontal cortex was consistently less severely involved than usually observed in Alzheimer's disease. This suggests that the distribution of the lesions had been shifted to specific elements of the visual system. In the present study, we report the quantitative analysis of a new case of Alzheimer's disease with possible Balint's syndrome and re-evaluate a case originally described in 1945. The distribution of lesions in these two cases parallels previous observations of Alzheimer's disease cases with early visual impairment. Both cases displayed very high densities of neurofibrillary tangles and senile plaques in the primary visual cortex, secondary visual cortex, visual association areas of the dorsal occipital and posterior parietal lobe and in the posterior cingulate cortex, whereas the prefrontal and inferior temporal regions were comparatively less affected. These cases may define clinical subgroups of Alzheimer's disease and suggest that the breakdown of corticocortical projections that is known to occur in dementia may involve select components of specific functional systems in certain cases. In particular, pathways that subserve motion detection and visuospatial analysis appear to be dramatically affected in these cases presenting with Balint's syndrome. Thus, Alzheimer's disease may be a more heterogeneous disorder than previously thought, and refined neuropsychological testing as well as detailed neuropathological evaluation may be of value to detect possible clinical variants of this dementing condition.

Key words: Alzheimer's disease – Balint's syndrome – Corticocortical projections – Neurofibrillary tangles – Posterior cortical atrophy

In recent years, several clinical and neuropathological studies have demonstrated the occurrence of Alzheimer's disease (AD) cases with atypical clinical presentations. Most of these cases presented with complex and variable disturbances of visual function [5, 6, 17, 20, 22, 23, 32, 35, 36]. Deficits in motion perception and target tracing are considered to be relatively common once dementia is established [26, 29, 31]. However, these particular cases are of special interest since visual symptomatology was the first clinical evidence of the degenerative process, preceding the memory impairment and cognitive deficits typically observed in AD. In a clinical study evaluating a population of demented people, some patients exhibited a slow progression of the dementia along with severe visual impairment appearing early in the course of the disease [5]. These patients were characterized by complex neurological symptoms including alexia, anomia, agraphia, transcortical sensory aphasia, as well as Balint's and Gerstmann's syndromes, with a preservation of memory until late in the development of their illness. The cortical atrophy, as demonstrated by computer-assisted tomography and magnetic resonance imaging, was predominant in the parieto-occipital areas [5], and some of these cases had clear posterior cortical atrophy at autopsy.

In this context, Balint's syndrome is of particular relevance since it has been documented in association with AD in several studies [6, 22, 23, 30, 38, 39]. In 1909, Reszö Bálint described a complex visual syndrome characterized by a cortical paralysis of visual fixation

* Supported by the Brookdale Foundation, and NIH grants AG06647 and AG05138 (to P.R.H. and J.H.M.), and by funds from the Robert H. and Monica Cole Foundation and Alzheimer's Disease Research, a program of the American Health Assistance Foundation (to A.P.O.)

Correspondence to: P. R. Hof (address see above)

associated with an optic ataxia and a disturbance of visual attention in patients with large bilateral parieto-occipital lesions [3]. Patients presenting with Balint's syndrome are unable to attend to and keep fixation on a specific point located in the peripheral visual field (ocular apraxia), they experience an inaccurate reaching toward a target under visual guidance (optic ataxia), and are also unable to see more than one object at a time, since only stimuli in the macular area are seen, although the global visual field is normal (simultanagnosia). The co-occurrence of AD and Balint's syndrome was first recognized in a patient reported by Grünthal in 1928 [19]. The clinical symptomatology presented by AD patients presenting with Balint's syndrome suggests that the early stages of the dementing process may involve select cortical pathways linking the primary visual occipital regions to the posterior parietal and cingulate visual association cortex [22, 23, 39].

The primary sensory and motor cortical areas have been shown to be less affected in the course of AD than neocortical association regions [1, 4, 7, 18, 20–24, 33, 39, 43, 45]. In particular the primary visual (striate) cortex displays usually low densities of neurofibrillary tangles (NFT) predominantly localized in layers II and III, whereas the parastriate and peristriate regions are characterized by a noticeable and progressive increase in NFT numbers in both supra- and infragranular layers [1, 7, 20–23, 33, 39]. Senile plaques (SP) and amyloid deposits are more evenly distributed among the occipital areas [1, 4, 7, 20–23, 33, 39], and exhibit a clear laminar pattern in the primary visual cortex [4, 7, 33], where they are concentrated in layer IV and form a sharp band-like pattern at the boundary between layers IV and V [4, 7]. These regional and laminar trends in lesion distribution suggest that specific components of the visual system are differentially affected in AD [7, 20, 22, 23, 39].

In a recent survey of a large collection of human brains, we analyzed a series of nine cases displaying prominent visual symptomatology as the first sign of mental decline. Eight of these cases presented with typical Balint's syndrome [22, 23], while the last case had apperceptive visual agnosia [20]. Neuropathologically, all these cases showed posterior cortical atrophy and had much higher NFT and SP densities in the occipital cortex than is usually observed in AD, whereas the prefrontal areas were less affected [20, 22, 23, 39]. This suggested that in these particular cases, AD affected predominantly certain components of the visual cortical pathways [20, 22, 23, 39]. In the present study, we report a neuropathological analysis of a new case of posterior cortical atrophy in a patient with presenile dementia and displaying some elements of the Balint's syndrome, and present a re-evaluation with immunohistochemical methods of a similar case briefly described in 1945 by Morel [38]. The quantitative analysis of these cases is compared with our previous results on Balint's syndrome in AD [22, 23].

Case reports

Case 1

This patient first began to complain of visual difficulties at the age of 50 in 1978. At that time she saw several ophthalmologists but no specific abnormalities of vision could be demonstrated. In 1983, she was first evaluated neurologically and her persistent complaint at this time continued to relate to visual impairment. She could not read and had difficulty identifying objects. It was noted during the course of examination that she could identify objects when they were presented directly in front of her but she was unable to find an object in the room when asked. Her extraocular movements appeared to be full and her ocular examination otherwise was normal. Initially these symptoms were considered to be possibly related to hysteria. Formal neuropsychological evaluation, however, revealed a mild general cognitive impairment with a modest deficit of recent memory. At that time her Cognitive Capacity Screening Examination (Mini-Mental Status Examination) yielded a score of 22/30 and it was proposed that the patient had a primary degenerative dementia of the Alzheimer type with an associated psychiatric syndrome. Additional studies included evidence for a mild degree of cerebral atrophy on computer-assisted tomography scans, and a moderate posterior slowing was present on EEG. The patient continued to decline and on further examination in 1986, it was suggested that the unusual visual deficit probably represented Balint's syndrome. At that time, increased abnormalities in her visual function were noted. Eye movements were limited to infrequent and rather saccadic motions without ever appearing to fix on any objects. The patient progressively deteriorated requiring nursing home placement at the age of 60. She died shortly thereafter in 1988 of bronchopneumonia and sepsis following an episode of intestinal obstruction.

Case 2

This patient has been reported in a brief communication by Morel in 1945 [38]. At the age of 55, the patient developed rapidly progressive visual disturbances, increasing difficulties in reading, and slight memory impairment. However, a series of ophthalmological examinations performed between 1935 and 1942 showed a normal visual field and no alteration of both retinas. The patient was admitted to the psychiatric hospital in 1942, where he presented with memory and language impairment, and severe visuomotor deficits. In particular, the patient was unable to follow objects moving laterally or away from him, and could reach fixation on these objects only with great difficulty. Large objects were only partially perceived. Moving sight from a fixation point to another target resulted in a series of extremely inaccurate saccades and smooth pursuit ocular movements were impossible. As the patient rapidly became severely demented, further testing of the visual function was no longer tenable. The patient died in 1943 at the age of 64 of bronchopneumonia and acute pyelonephritis.

Materials and methods

The brains of cases 1 and 2 were obtained at autopsy and were fixed by immersion in a 10% formalin solution. The clinical and neuropathological data were obtained from the clinical records of the attending physicians, the Department of Pathology, University of Tennessee Medical Center, Knoxville, the Department of Neurology, Vanderbilt University, Nashville (case 1), and the Department of Psychiatry, University of Geneva School of Medicine, Geneva, Switzerland (case 2). The right hemisphere was available from case 1 for this study, and almost the entire brain was obtained from case 2. In addition, the microscope slides used by Morel for his description of case 2 [38] were available from the collection of neuropathological materials at the Department of

Psychiatry, University of Geneva School of Medicine. This Department holds a collection of over 6000 human brains, and despite approximately 50 years of storage in formalin, materials from case 2 were in outstanding condition (Fig. 1). In both cases, the following areas were analyzed (numeration according to Brodmann's nomenclature [8]): 17, 18 (primary and secondary visual cortex) and 19 in the occipital cortex, 7b in the posterior parietal cortex, 23 in the cingulate cortex, 20 in the temporal cortex, 9 in the prefrontal cortex, the entorhinal cortex and hippocampus. From each tissue block, 30-μm-thick sections were cut on a cryostat and stained for routine neuropathological evaluation with modified thioflavine S [48], modified Globus [23, 48], Bielchowsky, Holzer, and Campbell-Switzer-Martin [9] techniques, as well as hematoxylin-eosin and cresyl violet. From each block, additional sections were processed with specific antibodies to the microtubule-associated protein tau or to the amyloid βA4 protein. Characterization and specificity of these antibodies has been fully documented elsewhere [11, 12, 16, 28]. Briefly, 30-μm-thick sections were incubated overnight at 4 °C with the anti-tau antibody at a dilution of 1:2000 or with the anti-amyloid βA4 protein antibody at a dilution of 1:4000. Following incubation, sections were processed by the avidin-biotin method using a Vectastain ABC kit (Vector Laboratories, Burlingame, Calif.), and diaminobenzidine as a chromogen, and were intensified in 0.005 % osmium tetroxide.

All the sections were systematically surveyed and lesions were counted using a computer-assisted image analysis system consisting of a Zeiss Axiophot photomicroscope equipped with a Zeiss MSP65 computer-controlled motorized stage, a high sensitivity MTI CCD72 video camera, a DEC 5000 workstation and Macintosh II microcomputer, and custom-designed morphometry software. All quantitative analyses were performed on sections stained with the antibodies to tau and amyloid βA4 proteins. On each slide, NFT and SP were counted under five 1-mm-wide cortical traverses in layers I–III, IV–VI separately in each area, except in area 17, where lesions were counted in layers I–III, IV, and V–VI, respectively, yielding a total area for quantification of 4 mm^2/cortical region. Traverses were always counted in regions where the tissue was cut perpendicular to the pial suface to avoid artifacts resulting from oblique sectioning of the cortical layers.

Results

The neuropathological examination of the brains of both cases revealed cortical atrophy predominating on the posterior parietal cortex and occipital lobe (Fig. 1). There was no evidence of infection, tumor, large vascular lesion or traumatic alteration. No atheromatous lesion was detected in any of the major cerebral vessels. Routine microscopic evaluation showed that both cases contained numerous NFT and SP throughout the entire cortical mantle. The hippocampal formation, including entorhinal cortex, was severely affected and lesion counts consistently met the criteria for the neuropathological diagnosis of AD [27]. In addition, there was no cortical microinfarct, in particular in the posterior parietal and occipital regions. In the neocortex of both cases, the distribution of NFT and SP was qualitatively comparable to previous descriptions of lesion localization in AD [1, 4, 7, 20–24, 33, 43, 45]. In particular, the distribution of NFT and SP was qualitatively similar to that reported in the detailed study by Braak and collaborators [7], (Figs. 1, 2). In neocortical association areas, NFT and SP exhibited a bilaminar distribution and were more numerous in layers II, III, V and VI. SP tended to be more frequent in the supragranular layers, whereas the infragranular layers had higher NFT densities. In the primary and secondary visual cortex, however, NFT predominated in layer III and SP were equally represented in layers II to IV.

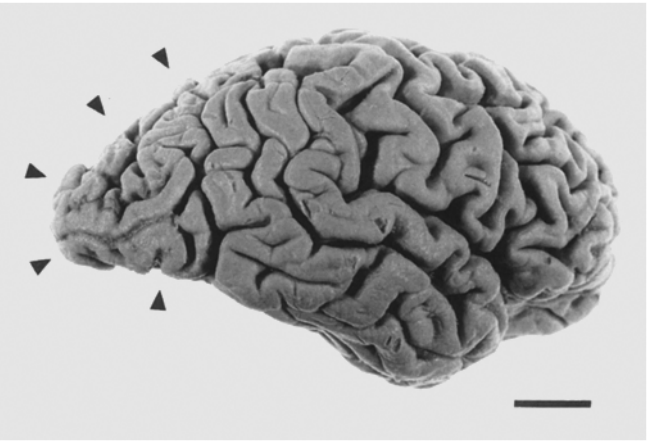

Fig. 1. Lateral view of the right hemisphere of case 2. Note the generalized cortical atrophy and the severe involvement of the occipital lobe (*arrowheads*). A view of the medial aspect of the left hemisphere of this case showing a comparable posterior cortical atrophy can be found in [38]. *Scale bar* = 2 cm

Table 1. Neurofibrillary tangle (NFT) counts in the neocortex of cases 1 and 2

Area		Case 1	Case 2
17			
Layers	I–III	80.6 ± 4.2	16.7 ± 1.9
	IV	7.2 ± 1.0	–
	V–VI	35.4 ± 2.2	9.7 ± 0.9
18			
Layers	I–III	150.6 ± 7.2	43.2 ± 2.9
	IV–VI	203.8 ± 9.3	50.6 ± 3.1
19			
Layers	I–III	239.2 ± 9.7	47.8 ± 3.0
	IV–VI	265.0 ± 6.9	55.2 ± 2.6
7b			
Layers	I–III	219.8 ± 11.4	89.8 ± 3.3
	IV–VI	243.4 ± 14.7	85.0 ± 2.2
23			
Layers	I–III	299.2 ± 6.3	52.4 ± 2.5
	IV–VI	292.2 ± 5.4	56.2 ± 2.0
20			
Layers	I–III	162.4 ± 10.1	34.6 ± 1.7
	IV–VI	216.0 ± 4.3	40.8 ± 1.6
9			
Layers	I–III	47.0 ± 4.3	33.4 ± 1.8
	IV–VI	83.8 ± 3.7	48.0 ± 2.6

The results represent means ± SEM and are expressed as NFT counts per mm of cortical traverse. Note the high NFT densities in the primary and secondary visual cortex in both cases. No NFT was detected in layer IV of area 17 in case 2. Also, NFT densities are higher in areas 19, 7b, and 23, whereas area 20 is relatively less affected. Area 9 shows a low NFT density in comparison to visual association regions. Areas are numbered according to Brodmann's nomenclature. Layers are indicated by Roman numerals. See text for details

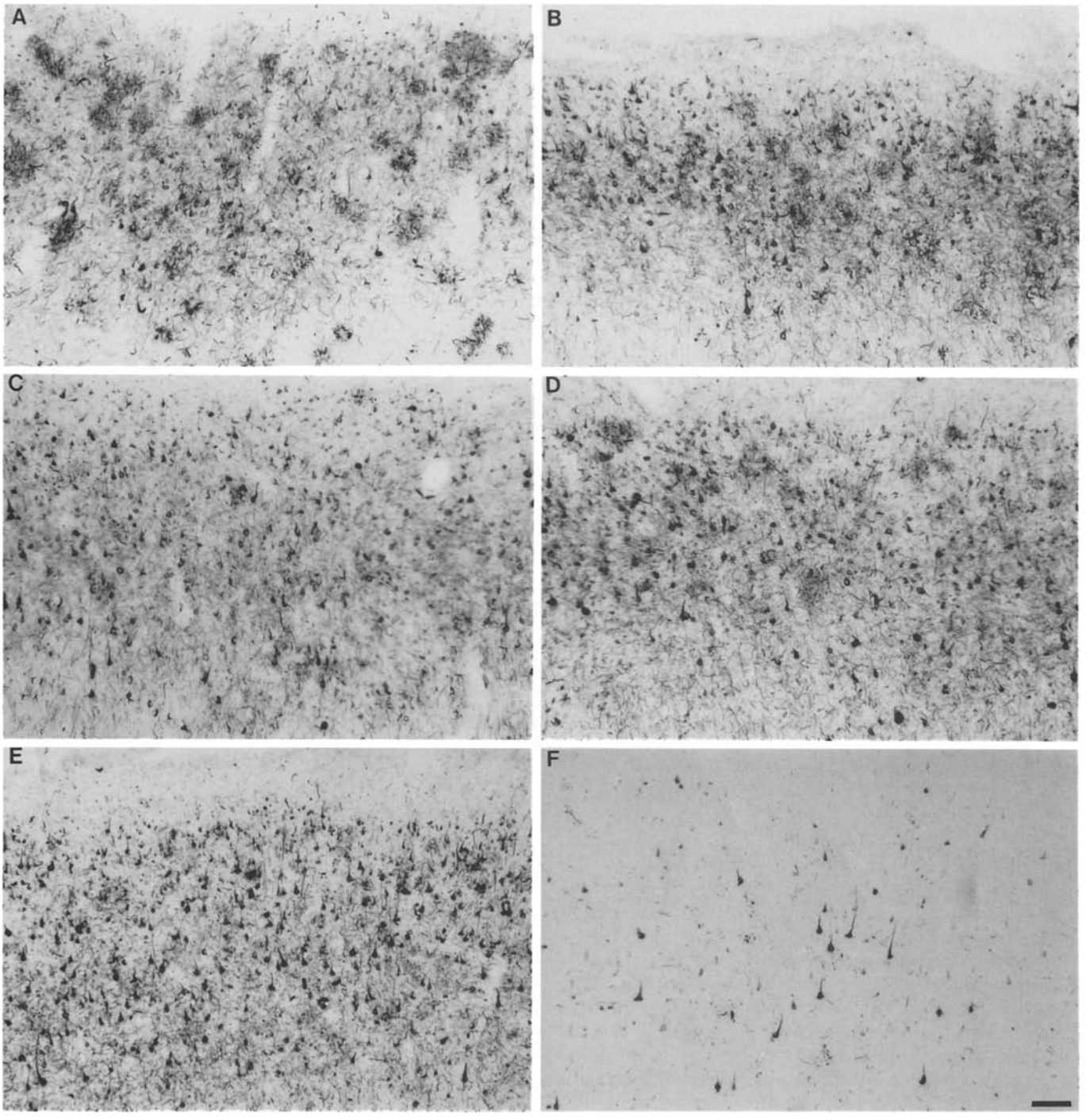

Fig. 2A–F. Distribution of neurofibrillary tangles (NFT) in the cerebral cortex of case 1. **A** Area 17 (primary visual cortex); note the very high NFT density. **B** Area 18 (secondary visual cortex). **C** Area 19 (dorsal occipital association cortex). **D** Area 7b (posterior parietal cortex). **E** Area 23 (posterior cingulate cortex). **F** Area 9 (prefrontal cortex). There is a progressive increase in NFT counts from area 18 to areas 7b and 23, whereas area 9 contains comparatively a lower NFT density. Note the very high density of neuropil threads in all of the areas, except area 9. Materials were stained with the antibody to the protein tau. *Scale bar* = 100 μm

Quantitatively, the densities and distribution of NFT and SP in these two cases were globally comparable to our previous findings in AD cases with Balint's syndrome [22, 23, 39]. Although there were large differences in NFT counts between cases 1 and 2, similar trends in NFT distribution and counts were observed in both cases. For instance in both cases, area 17 contained a high density of NFT (Table 1; Fig. 2A). There was a clear increase in NFT density from area 17 to the dorsally located visual association regions in the parietal cortex, as well as in the posterior cingulate cortex. The number of NFT was almost twice as high in area 18 as in area 17,

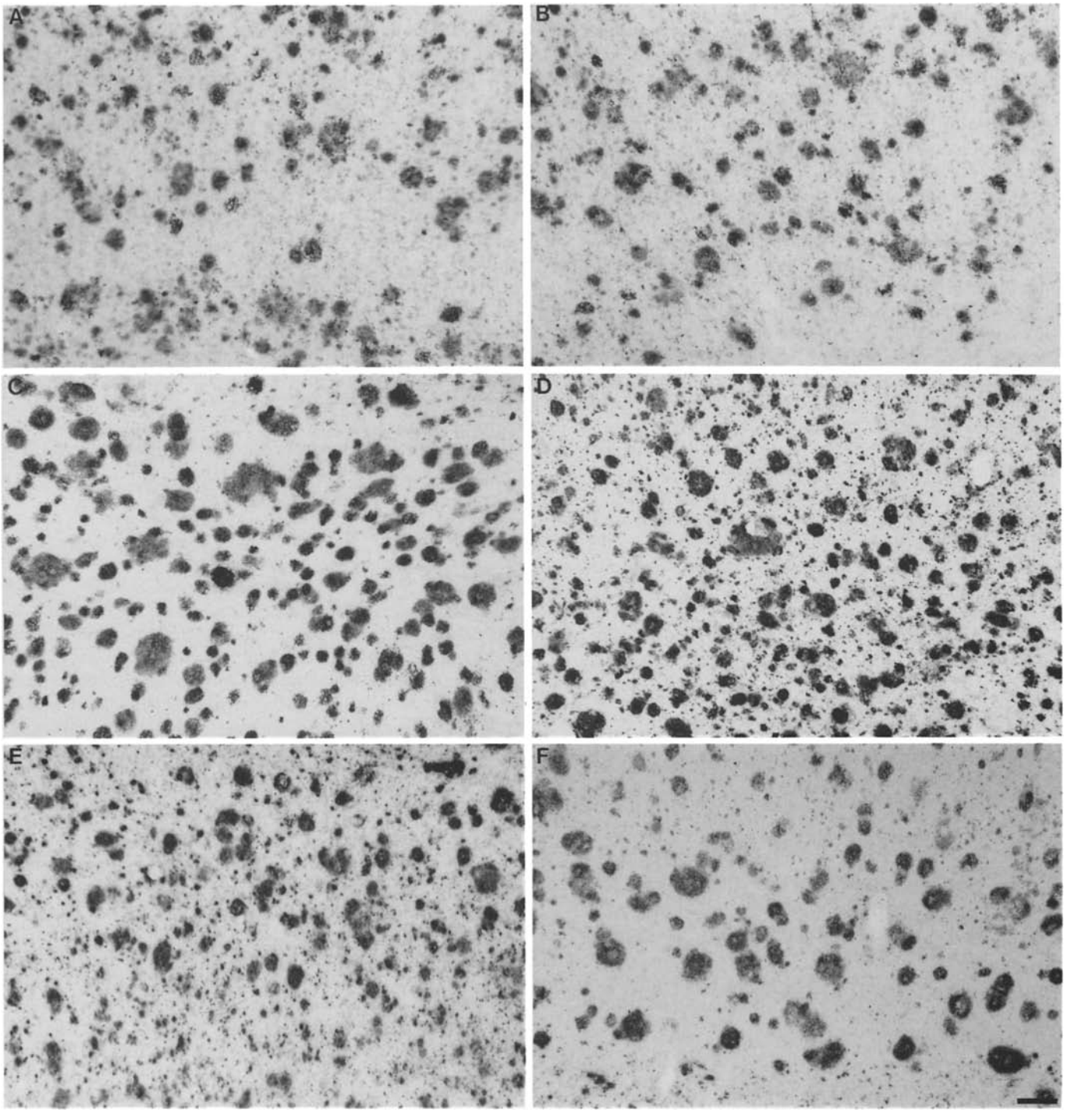

Fig. 3A–F. Distribution of senile plaques (SP) in the cerebral cortex. **A** Area 17 (primary visual cortex). **B** Area 18 (secondary visual cortex). **C** Area 19 (dorsal occipital association cortex). **D** Area 7b (posterior parietal cortex). **E** Area 23 (posterior cingulate cortex). **F** Area 20 (inferior temporal cortex). Note the very high SP densities in areas 18, 19, 7b and 23, whereas area 20 contains a relatively lower SP density. The well-defined band of SP at the bottom of panel (**A**) represents layer IVC of area 17 (see also [4, 7]). Materials were stained with the antibody to the amyloid βA4 protein. Microphotographs were all from case 1, except for areas 17 and 18 (**A,B**) which were obtained from case 2. *Scale bar* = 100 μm

and in both cases a further increase was observed in areas 19, 7b and 23 (Table 1, Fig. 2B–E). These progressive increases in NFT counts were present in both the supragranular and the infragranular layers. Areas 19, 7b and 23 had comparable NFT densities in case 1, whereas area 7b was the most severely affected region in case 2 (Table 1). Interestingly, the visual association region located in area 20 in the inferior temporal cortex, displayed lower NFT densities than areas 19, 7b and 23 (Table 1). In fact, in both cases, area 20 had NFT counts

comparable to those observed in the secondary visual cortex (area 18). Also, area 9 in the prefrontal cortex showed fewer NFT than the occipital, parietal and posterior cingulate regions (Table 1; Fig. 2F). In case 1, area 17 had 1.7-fold more NFT in layers I to III than area 9, and 2.4-fold more in layers V and VI. Similarly, in area 18 these differences with area 9 were 3.2-fold more NFT in layers I to III and 2.4-fold more in layers V and VI. The most striking differences in NFT counts with area 9 were observed in areas 19, 7b and 23, where they reached up to 6.4-fold in layers I to III and 3.5-fold in layers V and VI in area 23. In case 1, area 20 also had more NFT than area 9 with differences of 3.5-fold in layers I to III and 2.6-fold in layers V and VI. In case 2, areas 9 and 20 displayed comparable NFT counts, and although areas 19 and 23 contained more NFT than area 9, the only notable differences were seen in area 7b which had 2.7-fold more NFT than area 9 in layers I to III, and 1.8-fold more in layers V and VI. It should be noted that a comparable progressive increase in NFT density in areas 17, 18 and 19 was reported by Morel in his evaluation of case 2 [38]. Finally, all cortical regions except area 9 contained very high densities of neuropil threads and dystrophic profiles that were stained by the antibody to the microtubule-associated protein tau (Fig. 2).

Table 2. Senile plaque (SP) counts in the neocortex of cases 1 and 2

Area		Case 1	Case 2
17			
Layers	I–III	58.4 ± 3.3	77.2 ± 3.8
	IV	70.0 ± 3.4	45.8 ± 2.2
	V–VI	12.4 ± 1.9	55.2 ± 3.3
18			
Layers	I–III	109.0 ± 4.2	101.6 ± 3.3
	IV–VI	55.0 ± 3.6	69.1 ± 3.1
19			
Layers	I–III	160.2 ± 7.1	113.0 ± 6.8
	IV–VI	102.4 ± 3.9	73.4 ± 2.3
7b			
Layers	I–III	164.2 ± 6.2	121.4 ± 4.2
	IV–VI	131.4 ± 8.2	59.4 ± 3.4
23			
Layers	I–III	180.4 ± 4.0	129.0 ± 3.7
	IV–VI	107.2 ± 3.8	51.8 ± 2.6
20			
Layers	I–III	128.8 ± 7.3	76.6 ± 1.5
	IV–VI	64.2 ± 3.3	55.2 ± 1.7
9			
Layers	I–III	128.0 ± 7.3	67.6 ± 2.1
	IV–VI	74.6 ± 4.2	42.6 ± 3.8

The results represent means ± SEM and are expressed as SP counts per mm of cortical traverse. Note the high SP densities in the primary and association visual cortex in both cases. There are also more SP in the dorsally located visual association regions in areas 19 and 7b and in the posterior cingulate cortex than in area 20 in the temporal lobe and area 9 in the frontal lobe. Areas are numbered according to Brodmann's nomenclature. Layers are indicated by Roman numerals. See text for details

SP distribution also demonstrated progressive density increases from area 17 toward areas 19, 7b and 23, in both cases (Fig. 3A–E). Case 1 exhibited overall higher SP densities than case 2, except in area 17 where comparable counts were found in the two cases. In case 1, area 18 contained about twice as many SP as area 17 in layers I to III, and further increases were noted with areas 19 and 7b having comparable SP numbers (Table 2; Fig. 3B–D). Layers I to III of area 23 were characterized by very high SP densities (Table 2; Fig. 3E). A similar trend in SP distribution was found in case 2, where layers I to III of area 23 also contained the highest SP counts. Comparable increases in SP density were observed in the infragranular layers in the same regions (Table 2). In both cases, areas 9 and 20 had comparable SP densities in the supragranular and infragranular layers. Also, there were fewer SP in these areas than in area 18 in case 2, and in areas 19, 7b and 23 in both cases (Table 2; Fig. 3F). In addition, case 2 displayed similar SP numbers in area 17 as in areas 9 and 20, whereas lower values were observed in area 17 of case 1.

Discussion

The analysis of these two cases of AD with Balint's syndrome confirm and extend our previous observations on similar cases [20, 22, 23, 39]. Both cases 1 and 2 had large numbers of lesions not only in the primary and secondary visual areas, but also in visual association areas 19, 7b and 23. In addition, both cases displayed much higher lesion densities in visual areas than is usually observed in AD, as compared to data reported in quantitative analyses of AD cases [20–24, 33, 45]. Differences in NFT counts between cases 1 and 2 may be related to the fact that case 2 was kept in storage for about 50 years resulting in partial loss of immunoreactivity to certain epitopes, despite an apparent excellent preservation of the materials. However, case 2 still had higher NFT densities than previously documented AD cases in the primary and secondary visual cortex. For instance, Lewis and colleagues reported a mean of 0.9 NFT per 250-μm-wide cortical traverse across all layers in area 17, and a mean of 19.7 NFT in area 18 [33]. Similarly, mean values of 3.1 NFT per mm of cortical traverse in area 17, and 38.7 NFT in area 18 across all layers were inferred from the study of Hof and Morrison [21]. In addition, the present cases had generally more SP than was previously documented in AD patients with Balint's syndrome [22, 23, 39]. A possible explanation for this discrepancy is that previous analyses were performed on materials stained with an argentic impregnation which may be less reliable than immunohistochemistry for SP detection [48]. The present results confirm that regions located in the dorsal aspect of the occipital lobe, the posterior parietal, and the posterior cingulate cortex are more severely affected in this subgroup of demented patients than is usually seen in AD. The preferential distribution of NFT and SP in these areas could represent a displacement of the regional

lesion localization typically seen in AD, since areas 9 and 20 that are known to be dramatically affected in AD, appear to be less involved in these cases with Balint's syndrome than in demented cases without visual symptomatology. These observations also parallel recent clinicopathological analyses, showing a dramatic involvement of the occipital and parietal regions and fewer changes in the frontal cortex in patients presenting with either all of the features of Balint's syndrome [6] or elements of Balint's syndrome combined with other complex visual disturbances [32].

The functional implications of the atypical lesion localization and densities observed in AD cases with posterior cortical atrophy can be appreciated in considering the distribution of corticocortical pathways between the different visual areas in the occipital, parietal and temporal neocortex. Studies of the macaque monkey neocortex have demonstrated that the visual system consists of two major separate components: a pathway linking the primary visual cortex to the inferior temporal cortex that is primarily responsible for form and color detection, and a pathway linking the primary visual cortex with the posterior parietal cortex that subserves visuospatial functions and motion analysis [13, 15, 34, 37, 50, 54]. Assuming that visual function is distributed in a similar fashion onto specific connections in the human visual system, then the degree to which the distribution of the pathological changes in the AD cases with Balint's syndrome reflects a specific visual disconnection can be interpreted in comparison to the available data on corticocortical connections in monkey visual areas. Connection-tracing studies in the monkey neocortex have revealed that forward projections ascend a hierarchical system of connections proceeding from areas closer to the primary sensory input to more distant areas [e.g., V1 (area 17) to V2 (area 18), V2 to V3 and V4 (possible equivalents of area 19), and from there to association areas in the parietal, temporal and posterior cingulate cortex] [15, 44, 46, 49, 54]. Forward projections originate mostly from layer III pyramidal neurons and terminate primarily in layers III and IV. Feedback projections travel in the reverse direction in the hierarchical scheme, originate from pyramidal neurons in layers III, V and to a lesser degree VI, and terminate in layers I, II, V and VI [15, 49].

The distribution of pathological changes in the AD cases with Balint's syndrome suggests that along with an increased number of lesions in the primary visual cortex, these cases display a severe and specific disconnection of the projection between the primary visual cortex and the regions located in the posterior parietal cortex, whereas the pathway to the inferior temporal cortex is not more damaged than is usually observed in AD [20, 22, 23, 39]. In this context it is also interesting to note that in a case of AD presenting with an apperceptive visual agnosia as the first symptom of the dementing process, we found increased NFT and SP densities in the inferior temporal cortex, while the posterior parietal cortex was relatively spared [20]. Furthermore, the severe involvement of the posterior cingulate cortex in the cases with Balint's syndrome is of particular interest, since this cortical area constitutes a major component of the visuomotor system [40–42]. It is connected to the posterior parietal and dorsal occipital regions as well as to the hippocampal formation [2, 40–42, 51]. Neurons in the posterior cingulate region respond to specific eye position in the orbit and are phasically active during saccadic movements [40–42]. The anatomic position of the posterior cingulate cortex between the hippocampal formation and the regions of neocortex involved in visuospatial tasks suggests that it plays a key role in visuospatial cognition [40, 42]. In addition, recent studies have shown that the posterior cingulate cortex is affected relatively late in the progression of AD and exhibits a great variability across cases in lesion densities [52, 53]. Thus, the early involvement of this cortical region may represent a key factor in the development of visuomotor disturbances in dementia. The notion that the involvement of the occipital, posterior parietal and posterior cingulate regions occurred early in the course of the disease in the cases with Balint's syndrome is also supported by the fact that the prefrontal cortex of these cases had fewer lesions than is usually observed in AD. In addition, the inferior temporal cortex and hippocampal formation had lesion densities comparable to those observed in AD cases.

It has been proposed that in AD a certain number of SP may originate from axonal fibers and terminals from neurons that contain NFT [21, 23, 24, 33, 43, 45]. According to this scheme, the distribution of NFT and SP in the cases with Balint's syndrome suggests that many specific elements of these cortical circuits are profoundly disrupted. For instance, the heightened density of NFT in layer III of area 17 in these cases indicates that the projection to area 18 is affected. The high density of NFT in layer III of area 18 suggests that the forward projections to dorsal area 19, and to area 7b are affected in the cases with Balint's syndrome. In addition, the high density of NFT in layers V and VI of area 18 suggests that the feedback projection to 17 is also disrupted. The disruption of this projection that terminates in both supra- and infragranular layers may explain the large SP counts in all layers of area 17 in the cases with Balint's syndrome. The increase in SP density in area 18 may reflect the involvement of terminals from feedback corticocortical projections from area 19, as well as forward projections from area 17. Finally, the very high SP number in posterior parietal cortex and posterior cingulate cortex is likely to reflect the degeneration of the terminals from forward projections originating in dorsal area 19 and related occipito-parietal visual areas. Thus, even though cases with Balint's syndrome may represent a variant of AD with a specific distribution of the pathological changes along select components of the visual system, the present data confirm that AD involves the breakdown of specific corticocortical projections subserved by subsets of highly vulnerable pyramidal neurons [21, 24, 33, 39].

These isolated observations may indicate that AD is in fact an heterogeneous disorder and may exhibit system-specific manifestations early in the progression of the symptomatology. In this respect, it is worth noting

that rare cases with parietal lobe syndrome, somatosensory and primary motor impairment have also been reported [10, 18, 25]. The cases with motor and somatosensory dysfunction displayed heightened lesion densities in the primary motor and primary sensory areas of the neocortex [18, 25]. Thus, certain cases of dementia clearly do not correspond to the accepted clinical and neuropathological criteria for the definition of AD, yet they show the same histopathological lesions [14]. Such cases may define possible clinical subgroups of AD and stress the necessity for detailed and accurate neuropsychological testing, as well as for meticulous neuropathological assessment of dementing syndromes.

Acknowledgements. We thank M. Surini and R. S. Woolley for expert technical assistance, Drs. A. Delacourte and N. K. Robakis for generous provision of the antibodies to tau and amyloid βA4 proteins, Drs. R. C. Switzer and S. K. Campbell and the staff of the Department of Pathology at the University of Tennessee Medical Center for technical and clinical support, Dr. W. G. Young and S. Gong for software development, and E. A. Nimchinsky for critical reading of the manuscript.

References

1. Arnold SE, Hyman BT, Flory J, Damasio AR, Van Hoesen GW (1991) The topographical and neuroanatomical distribution of neurofibrillary tangles and neuritic plaques in the cerebral cortex of patients in Alzheimer's disease. Cerebral Cortex 1:103–116
2. Baleydier C, Mauguière F (1987) Network organization of the connectivity between parietal area 7, posterior cingulate cortex and medial pulvinar nucleus: a double fluorescent tracer study in monkey. Exp Brain Res 66:385–393
3. Bálint R (1909) Seelenlähmung des "Schauens", optische Ataxie, räumliche Störung der Aufmerksamkeit. Monatsschr Psychiatr Neurol 25:51–81
4. Beach TG, McGeer EG (1992) Senile plaques, amyloid β-protein, and acetylcholinesterase fibres: laminar distributions in Alzheimer's disease striate cortex. Acta Neuropathol 83:292–299
5. Benson DF, Davis RJ, Snyder BD (1988) Posterior cortical atrophy. Arch Neurol 45:789–793
6. Berthier ML, Leiguarda R, Starkstein SE, Sevlever G, Taratuto AL (1991) Alzheimer's disease in a patient with posterior cortical atrophy. J Neurol Neurosurg Psychiatry 54:1110–1111
7. Braak H, Braak E, Kalus P (1989) Alzheimer's disease: areal and laminar pathology in the occipital isocortex. Acta Neuropathol 77:494–506
8. Brodmann K (1909) Vergleichende Lokalisationslehre der Grosshirnrinde in ihren Prinzipien dargestellt auf Grund des Zellenbaues. Barth, Leipzig
9. Campbell SK, Switzer RC, Martin TL (1987) Alzheimer's plaques and tangles: a controlled and enhanced silver-staining method. Soc Neurosci Abstr 13:678
10. Crystal HA, Horoupian DS, Katzman R, Jotkowitz S (1982) Biopsy-proved Alzheimer disease presenting as a right parietal lobe syndrome. Ann Neurol 12:186–188
11. Défossez A, Beauvillain JC, Delacourte A, Mazzuca M (1988) Alzheimer's disease: a new evidence for common epitopes between microtubule associated protein tau and paired helical filaments (PHF): demonstration at the electron microscope by a double immunogold labelling. Virchows Arch [A] 413:141–145
12. Delacourte A, Flament S, Dibe EM, Hublau P, Sablonnière B, Hémon B, Scherrer V, Défossez A (1990) Pathological proteins tau 64 and 69 are specifically expressed in the somatodendritic domain of the degenerating cortical neurons during Alzheimer's disease: demonstration with a panel of antibodies against tau proteins. Acta Neuropathol 80:111–117
13. DeYoe EA, Van Essen DC (1988) Concurrent processing streams in monkey visual cortex. Trends Neurosci 11:219–225
14. Engel PA, Vinters HV, Grunnet M (1992) Alzheimer's disease of plaque disease? Two cases at the frontier of a definition. J Geriatr Psychiatry Neurol 5:200–209
15. Felleman DJ, Van Essen DC (1991) Distributed hierarchical processing in the primate cerebral cortex. Cerebral Cortex 1:1–47
16. Flament S, Delacourte A, Delaère P, Duyckaerts C, Hauw JJ (1990) Correlation between microscopical changes and tau 64 and 69 biochemical detection in senile dementia of the Alzheimer type. Tau 64 and 69 are reliable markers of the neurofibrillary degeneration. Acta Neuropathol 80:212–215
17. Fletcher WA, Sharpe JA (1988) Smooth pursuit dysfunction in Alzheimer's disease. Neurology 38:272–277
18. Golaz J, Bouras C, Hof PR (1992) Motor cortex involvement in presenile dementia: report of a case. J Geriatr Psychiatry Neurol 5:85–92
19. Grünthal E (1928) Zur hirnpathologischen Analyse der Alzheimerschen Krankheit. Psychiatr Neurol Wochenschr 36:401–407
20. Hof PR, Bouras C (1991) Object recognition deficit in Alzheimer's disease: possible disconnection of the occipitotemporal component of the visual system. Neurosci Lett 122:53–56
21. Hof PR, Morrison JH (1990) Quantitative analysis of a vulnerable subset of pyramidal neurons in Alzheimer's disease. II. Primary and secondary visual cortex. J Comp Neurol 301:55–64
22. Hof PR, Bouras C, Constantinidis J, Morrison JH (1989) Balint's syndrome in Alzheimer's disease: specific disruption of the occipito-parietal visual pathway. Brain Res 493:368–375
23. Hof PR, Bouras C, Constantinidis J, Morrison JH (1990) Selective disconnection of specific association pathways in cases of Alzheimer's disease presenting with Balint's syndrome. J Neuropathol Exp Neurol 49:168–184
24. Hof PR, Cox K, Morrison JH (1990) Quantitative analysis of a vulnerable subset of pyramidal neurons in Alzheimer's disease. I. Superior frontal and inferior temporal cortex. J Comp Neurol 301:44–54
25. Jagust WJ, Davies P, Tiller-Borcich JK, Reed BR (1990) Focal Alzheimer's disease. Neurology 40:14–19
26. Katz B, Rimmer S (1989) Ophthalmologic manifestations of Alzheimer's disease. Surv Ophthalmol 34:31–43
27. Khachaturian ZS (1985) Diagnosis of Alzheimer's disease. Arch Neurol 42:1097–1105
28. Kim KS, Miller DL, Sapienza VG, Chen CJ, Vai C, Grundke-Iqbal I, Curry JR, Wisniewski HM (1988) Production and characterization of monoclonal antibodies reactive to synthetic cerebrovascular amyloid peptide. Neurosci Res Commun 2:121–130
29. Kiyosawa M, Bosley TM, Chawluk J, Jamieson D, Schatz NJ, Savino PJ, Sergott RC, Reivich M, Alavi A (1989) Alzheimer's disease with prominent visual symptoms – Clinical and metabolic evaluation. Ophthalmology 96:1077–1086
30. Kobayashi S, Hirota N, Saito K, Utsuyama M (1987) Aluminum accumulation in tangle-bearing neurons of Alzheimer's disease with Balint's syndrome in a long-term aluminum refiner. Acta Neuropathol (Berl) 74:47–52
31. Kuskowski MA, Malone SM, Mortimer JA, Dysken MW (1989) Smooth pursuit eye movements in dementia of the Alzheimer type. Alzheimer Dis Assoc Disord 3:157–171
32. Levine DN, Lee JM, Fisher CM (1993) The visual variant of Alzheimer's disease: a clinicopathologic case study. Neurology 43:305–313

33. Lewis DA, Campbell MJ, Terry RD, Morrison JH (1987) Laminar and regional distribution of neurofibrillary tangles and neuritic plaques in Alzheimer's disease: a quantitative study of visual and auditory cortices. J Neurosci 7:1799–1808
34. Livingstone M, Hubel D (1988) Segregation of form, color, movement, and depth: anatomy, physiology, and perception. Science 240:740–749
35. Mendez MF, Mendez MA, Martin R, Smyth KA, Whitehouse PJ (1990) Complex visual disturbances in Alzheimer's disease. Neurology 40:439–443
36. Mendez MF, Turner J, Gilmore GC, Remler B, Tomsak RL (1990) Balint's syndrome in Alzheimer's disease: visuospatial functions. Int J Neurosci 54:339–346
37. Mishkin M, Ungerleider LG, Macko KA (1983) Object vision and spatial vision: two cortical pathways. Trends Neurosci 6:414–417
38. Morel F (1945) Les aires striée, parastriée et péristriée dans les troubles de la fonction visuelle au cours de la maladie d'Alzheimer. Confin Neurol 6:238–242
39. Morrison JH, Hof PR, Bouras C (1991) An anatomic substrate for visual disconnection in Alzheimer's disease. Ann NY Acad Sci 640:36–43
40. Olson CR, Musil SY (1992) Posterior cingulate cortex: sensory and oculomotor properties of single neurons in behaving cat. Cerebral Cortex 2:485–502
41. Olson CR, Musil SY (1992) Topographic organization of cortical and subcortical projections to posterior cingulate cortex in the cat: evidence for somatic, ocular and complex subregions. J Comp Neurol 323:1–24
42. Olson CR, Musil SY, Goldberg ME (1993) Neurophysiology of posterior cingulate cortex in the behaving monkey. In: Vogt BA, Gabriel M (eds) The neurobiology of cingulate cortex and limbic thalamus. Birkhäuser, Boston (in press)
43. Pearson RCA, Esiri MM, Hiorns RW, Wilcock GK, Powell TPS (1985) Anatomical correlates of the distribution of the pathological changes in the neocortex in Alzheimer's disease. Proc Natl Acad Sci USA 82:4531–4534
44. Rockland KS, Pandya DN (1979) Laminar origins and terminations of cortical connections of the occipital lobe in the rhesus monkey. Brain Res 179:3–20
45. Rogers J, Morrison JH (1985) Quantitative morphology and regional and laminar distribution of senile plaques in Alzheimer's disease. J Neurosci 5:2801–2808
46. Tigges J, Tigges M, Anschel C, Cross NA, Letbetter WD, McBride RL (1981) Areal and laminar distribution of neurons interconnecting the central visual areas 17, 18, 19 and MT in the squirrel monkey (*Saimiri*). J Comp Neurol 202:481–490
47. Tusa RJ, Ungerleider LG (1988) Fiber pathways of cortical areas mediating smooth pursuit eye movements in monkeys. Ann Neurol 23:174–183
48. Vallet PG, Guntern R, Hof PR, Golaz J, Delacourte A, Robakis NK, Bouras C (1992) A comparative study of histological and immunohistochemical methods for neurofibrillary tangles and senile plaques in Alzheimer's disease. Acta Neuropathol 83:170–178
49. Van Essen DC (1985) Functional organization of primate visual cortex. In: Peters A, Jones EG (eds) Cerebral cortex, vol 3, Visual cortex. Plenum Press, New York, pp 259–329
50. Van Essen DC, Maunsell JHR (1983) Hierarchical organization and functional streams in the visual cortex. Trends Neurosci 6:370–375
51. Vogt BA, Pandya DN (1987) Cingulate cortex of rhesus monkey. II. Cortical afferents. J Comp Neurol 262:271–289
52. Vogt BA, Van Hoesen GW, Vogt LJ (1990) Laminar distribution of neuron degeneration in posterior cingulate cortex in Alzheimer's disease. Acta Neuropathol 80:581–589
53. Vogt BA, Crino PB, Vogt LJ (1992) Reorganization of cingulate cortex in Alzheimer's disease: neuron loss, neuritic plaques, and muscarinic receptor binding. Cerebral Cortex 2:526–536
54. Zeki SM, Schipp S (1988) The functional logic of cortical connections. Nature 335:311–317